

Research article

Polymeric nanoparticle encapsulating Docetaxel for prolonged and targeted delivery to breast cancer

Mufassir Momin, Zahid Zaheer*, Rana Zainuddin, Jaiprakash N. Sangshetti

Dept. of Quality Assurance, Y.B. Chavan College of Pharmacy, Dr. Rafiq Zakaria Campus, Aurangabad 431001, Maharashtra, India.

Key words: Hyaluronic acid, Chitosan, Docetaxel, Breast cancer, Cytotoxicity, Tumour inhibition.

***Corresponding Author:** Zahid Zaheer, Department of Quality Assurance, Y. B. Chavan College of Pharmacy, Dr. Rafiq Zakaria Campus, Aurangabad, 431001, Maharashtra, India.

Abstract

Chitosan nanoparticles (HA-CHI-NP) containing docetaxel (DTX) were prepared, by ionotropic gelation method and further coupled with hyaluronic acid for targeting effect, in the treatment of breast cancer. Nanoparticles (NP's) have been characterized for the particle size, stability and shape with the help of zeta sizer, zeta potential and SEM. NP's were found to be spherical in shape and the size were around 97.36 ± 3.07 nm with 0.5 polydispersity index. NP's were also characterized for FTIR, DSC and PXRD. The *in-vitro* drug release of plain DTX and docetaxel loaded chitosan nanoparticle (DTX-CHI-NP) revealed higher and prolonged release of drug from DTX-CHI-NP than with plain DTX. *In-vitro* cytotoxicity was assessed by MTT assay using MCF-7 cell lines at different concentration (5, 10, 25, 50 and 100 $\mu\text{g/ml}$) and time intervals (24, 48 and 72h). Higher inhibitory effect of DTX-CHI-NP was observed with an IC_{50} value of approximately 2.18 $\mu\text{g/ml}$ at 72h. The formulation was also assessed for pharmacokinetic profile, biodistribution and tumour inhibition effect.

Introduction

Chemotherapy is widely used for the treatment of cancers, but the clinical effectiveness of chemotherapy is limited by significant side effects of chemotherapeutic agents and resistance generated by the cancerous tissues to limit their use [1]. Conventional delivery of chemotherapeutic agents is nonspecific and is toxic to normally dividing cells. It might cause, cardiotoxicity, kidney damage, and immunosuppression, leading to therapeutic failure of therapy and death. Moreover, the phenomenon of multidrug resistance (MDR), may further limit the success of the chemotherapy treatment. Due to the MDR effect the therapeutic index of the administered drugs are highly reduced as a result of the drugs being pumped out of the cells prior to achieving intracellular therapeutic functions. One strategy to increase drug selectivity toward cancer cells and to overcome resistance is to deliver antitumor compounds using targeted nanoparticulate carrier system. Docetaxel and doxorubicin are widely used in the treatment of a several solid tumour, however, associated with various severe toxicity [2-5]. Targeting moieties and acid-labile linkages in the structure of nanoparticulate delivery system can be a effective cancer treatment [6]. The DTX polymeric micelles as carriers have shown promising results in cancerous patient [7].

The solutions to all the above mentioned critical factors developed by the researchers are to focus on effectively delivery of drugs to tumor sites with maintained or improved therapeutic potency. Nanoparticulate carriers

system have received much attention due to the crucial properties of tumor-targeting, reduced drug resistance, and improved delivery of drugs with low water solubility [8]. To improve tumor targeting and cellular uptake, NPs can also be functionalized with active targeting molecules, such as antibodies, antibody fragments, small molecules, or peptides [9]. The incorporation of active targeting ligands is designed to improve and enhance NP accumulation at the tumor site. The active targeting approach for the delivery of anticancer drug exploits specific interactions between receptors on the cell surface and targeting moieties conjugated to the polymer NP. The active targeting strategy displays enhanced permeability and retention (EPR) effect, with the increases in the therapeutic index through receptor mediated uptake by targeting cancer cells [10, 11]. The antitumor efficacy of targeting NPs is significantly influenced by intracellular trafficking pathways. Therefore, in addition to binding capability, targeting ligands also exert a strong influence on intracellular signaling cascades may be expected to improve the therapeutic efficacy of active targeting NP [9].

Hyaluronic acid, a linear polysaccharide of alternating d-glucuronic acid (GlcUA) and N-acetyl-d-glucosamine (GlcNAc) units, serves a variety of extracellular functions. These include direct receptor mediated effects on cell adhesion, growth and migration and as a signaling molecule in cell motility, wound healing, inflammation and cancer metastasis. These effects occur via intracellular signaling pathways in which HA binds and gets internalized by cell-surface receptors. Most

malignant solid tumors and their surroundings to normal tissue contain elevated levels of HA and these high levels of HA production provide a matrix that facilitates invasion [12]. Isoforms of HA receptors, CD44 and RHAMM are also over expressed in transformed human breast epithelial cells, colorectal carcinoma and other cancers. As a result, malignant cells with the highest metastatic potential often show enhanced binding and internalization of HA [13].

Chitosan (CHI) is a natural polymer with extensive applications in biomedical field such as in drug delivery, wound healing, less preparation time making it useful for gene delivery, protein and peptide delivery. Hence CHI was used for the preparation of DTX NP for a targeted delivery to breast carcinoma. Docetaxel (DTX) is used in the treatment of breast, lung, ovarian, head and neck, urothelial, pancreatic and gastric carcinoma as a microtubule polymerization inhibitor. Because of the bulky, extended fused ring with several hydrophobic substitutes in chemical structure, DTX is commonly administered parenterally but produces severe toxic effects of gastrointestinal, hematological, neural, cardiac, and dermatological origin. Site-specific delivery of DTX may reduce the systemic side effects and provide effective and safe therapy of breast cancer that may reduce the dose and duration of therapy when compared with the conventional therapy (TAXOTERE). Tween 80 used frequently causes hypersensitivity reactions such as hypotension, bronchospasm and urticaria. Also, it hampers the clinical usefulness because of its haemolytic and viscosity [14]. In order to eliminate the Tween 80-based vehicle and to increase DTX solubility, alternative dosage forms have been suggested including liposomes [16,17] as well as design of water-soluble prodrugs, use of additives such as complexing agents [18, 19], co-solvents [20], surfactants [21] or a combination effect of any of the above [22].

In this study, HA coupled CHI-NP was prepared by ionic gelation method with chitosan, TPP and hyaluronic acid. The obtained NP's were characterized for the shape, particle size, zeta potential, drug entrapment efficiency and *in-vitro* drug release. The *in-vitro* cytotoxicity study was also performed on MCF-7 cell lines of human breast cancer. To assess the targeting property of HA coupled DTX-CHI-NP, biodistribution study and tumour inhibition study has been performed. The main pharmacokinetic parameters were calculated using trapezoidal method.

Experimental

Materials

Docetaxel hydrochloride (DTX) was a kind gift from Cipla Pharmaceuticals Pvt. Ltd. (Mumbai, India). Chitosan was purchased from Sigma-Aldrich Co., St. Louis, MO, USA. Sodium tripoly-phosphate,

Ethylenediamine-tetra acetic acid (EDTA) and dimethyl sulphoxide (DMSO) were purchased from Sigma-Aldrich Co., St. Louis, MO, USA. MCF-7 (human breast cancer adenocarcinoma) cell lines was purchased from NCCS, Pune, India. RPMI 1640 medium, membrane filter (MWCO 12000 Da) were purchased from Hi-Media Laboratories Pvt. Ltd. Mumbai, India. 1-ethyl-3-(3-dimethylamino-propyl) carbodiimide (EDC), Potassium dihydrogen phthalate and Potassium dihydrogen phosphate were purchased from Merck Life Science Pvt Ltd, (Mumbai, India). High-Performance Liquid Chromatography (HPLC) grade reagents such as acetonitrile were obtained from S. D. Fine-chem Ltd, Mumbai. Methanol was purchased from Merck & Co., Inc. (Mumbai, India). All other chemicals used were of analytical grade.

Preparation of DTX-CHI-NP's

Chitosan nanoparticles (CHI-NP's) were prepared according to the procedure described by Calvo *et al.* (1997) [24], with suitable modifications based on the ionotropic gelation method. CHI was dissolved in (2.0 mg/ml) aqueous acetic acid (0.75% v/v) (pH 4.0) solution kept on stirring on magnetic stirrer. TPP was dissolved in deionised water (1.0 mg/ml) and drug was added to TPP solution (10% w/v) and magnetically stirred (Remi 10ML DX, Mumbai, India) for 5 min. The drug/TPP solution was added to 4 ml of the CHI solution through a syringe needle under magnetic stirring at room temperature there by leading to formation of DTX loaded chitosan TPP nanoparticles (DTX-CHI-NP's). The dispersion formed was centrifuged (Hitachi, Himac CP100 MX, Japan) at 10,000 rpm at 4°C for 30 min. The sediment was poured in to dialysis bag (MWCO 10000) and dialyzed three times with phosphate buffer saline (pH 7.4) under strict sink conditions for 10 min to remove free drug from the formulation. The un-entrapped drug was estimated from supernatant and washings of formulation, spectrophotometrically at 230 nm (UV-1601, Shimadzu, Japan) to determine indirectly the amount of drug loaded in NP's. The dialyzed formulation was lyophilized [13, 23, 24].

Conjugation of DTX-NP with HA

Hyaluronic acid was coupled with preformed NP by forming a covalent bond between amino group of chitosan NP and carboxyl group of HA using EDC as coupling agent [28]. Briefly, DTX-CHI-NPs were suspended into PBS (pH 7.4) containing HA (NPs/HA ratio: 100:10 w/w). EDC (20 mg/ml of NPs/HA mixture) was added and vortexed and incubated for 2h at room temperature. The HA coupled NP's were separated from unconjugated HA using mini-column centrifugation (Sephadex G-75 packed column) technique and washed thrice with deaerated distilled water. The nanoparticles were collected after ultracentrifugation (Hitachi, Himac

CP100 MX, Japan) at 60,000 rpm for 45 min and were re-dispersed in distilled water for further lyophilization (Hetero Lyo. Pro. Model NO. 3000) at 4°C and these nanoparticles were termed as HA-DTX chitosan nanoparticles (HA-DTX-NP).

Drug entrapment

The contents of DTX entrapped in the CHI-TPP-NP dispersions were determined by high-performance liquid chromatography (HPLC). The drug entrapment efficiency (EE) and drug loading (DL) were calculated using the HPLC data as follows:

$$\text{Percent Entrapment Efficiency} = \frac{\text{Amount of drug entrapped}}{\text{Total amount of drug added}} \times 100$$

Physicochemical characterization

The size, polydispersity index (PDI) and zeta potential of HA-DTX-NP's were measured by dynamic light scattering (DLS) technique on a Malvern Zeta Sizer TM Nano ZS90 (Malvern Instruments Ltd, Malvern, UK) at room temperature. Samples were suitably diluted with HPLC grade water before measurement.

The FTIR spectra of DTX, NP's and HA-DTX-NP were obtained using a Jasco-2000 spectrophotometer, to understand interaction between DTX and NP. The spectra were obtained on KBr pellets in the region from 4000 cm⁻¹ to 400 cm⁻¹.

DSC study was performed to assess the thermal behavior and entrapment of drug into the CHI-TPP-NP. Thermal pattern of plain DTX and HA-DTX-NP was performed using DSC instrument (Mettler Toledo DSC 822e) in the range of ± 350 mW at RT with heating rate of 10°C/min in 25–500°C temperature range. A standard aluminum empty pan was used as reference standard. Analysis was performed in triplicate on 10 mg samples under nitrogen purge.

Molecular arrangement of drug in NP's was compared by powder X-ray diffraction patterns acquired at room temperature on X-ray diffractometer. Powder X-ray diffraction (PXRD) patterns of plain DTX and HA-DTX-NP were recorded with an X-ray diffractometer D8 Advanced Diffractometer, Bruker AXS GmbH, Germany) employing Cu K α (wavelength 1.5406 Å, tube operated at 40 kV, 40 mA) at room temperature. Data was collected over an angular range from 4 to 40° 2 θ at a step size of 0.01° and scan rate of one second. The obtained diffractograms were analyzed with DIFFRAC plus EVA (ver.9.0) diffraction software [25].

The CHI-TPP-NP's were characterized for their shape and morphology by using scanning electron microscope (JEOL Model JSM-6390LV).

Stability studies

HA-DTX-NP was stored in an aluminium stoppered vial and kept for stability testing at 60°C /75% RH for 1, 2, 3

and 6 months. The changes in particle size, FTIR peaks, DSC thermogram and encapsulation efficiency of the formulation were observed by analyzing the samples every month for 6 months (Data not shown) [26].

Drug release

The release profile of DTX from HA-DTX-NP was evaluated into a centrifugal tube containing 30 ml of phosphate buffer saline (PBS, pH 7.4) as a release media. The system was maintained at 37°C, with stirring rate of 100 rpm. The release media (0.2 ml) was sampled at predetermined time intervals (1, 2, 3, 4, 6, 8, 12, 16, 24, 36, 48, 60h) and replaced with an equal volume of PBS. The concentration of DTX was determined using high-performance liquid chromatography HPLC system (Agilent 1100) equipped with a G1311A pump and a G1313A auto-injector was used. Analysis was done using reversed phase GRACE C18 (4.6 mm × 25 cm, 5 μ m), UV-visible detector was at 230 nm, and the injection volume was 20 μ L. The analytical column was protected by a 2 μ m in-line filter frit (Upchurch Scientific, Oak Harbor, WA, USA) and the flow rate was 1 mL/min. The mobile phase consisted of Acetonitrile/deionized water (48/52, v/v) which was run isocratically.

Cytotoxicity study

The cytotoxicity of DTX and DTX-CHI-NP's to MCF-7 cell line was evaluated by MTT method. MCF-7 cells were plated at a density of 2×10⁴ cells per well in 100 ml of RPMI 1640 medium, containing 10% FBS, penicillin (100 IU.ml⁻¹) and streptomycin (100 μ gml⁻¹) in a humidified, 5% CO₂ incubator at 37°C. The cells were harvested using 0.25% trypsin with 0.02% EDTA when grown up to 80–90%.in 24-well plates and grown for 24h. Cells were then exposed to a series of DTX-CHI-NP at different concentrations (5, 10, 25, 50, 100 μ g/ml), for different time points (24, 48, 72h). The viability of cells was measured using the MTT method (n=5) [27].

Pharmacokinetic study

The pharmacokinetic study was performed on female Sprague Dawley rats which were divided into three groups (control, DTX group and DTX-CHI-NP group) and fasted for overnight prior to the experiments. Before experiment the rats were maintained at normal regular day and night exposure at 25±2°C and 50–60% relative humidity. The rats were anesthetized with diethyl ether. For comparison of bioavailability, the rats were administered with plain DTX and DTX-CHI-NP at a dose of 10 mg/kg intravenously. Serial blood samples (0.5 mL) were collected from the right femoral artery at specified intervals. The blood samples were centrifuged at 3000 × g for 10 min, and the plasma was then separated. Plasma sample (200 μ l) was mixed with 2 ml of acetonitrile and was centrifuged at 3000 × g for 10 min and the supernatant was separated and subjected to

centrifugation and then evaporated at 40°C. The residue obtained after the evaporation was reconstituted with 100 µL of mobile phase and quantified by HPLC (Agilent 1100) equipped with a G1311A pump and a G1313A auto-injector was used. The column was GRACE C18 (4.6 mm × 25 cm, 5 µm), UV-visible detector was at 230 nm with a flow rate of 1.0 mL/min. The parameters included plasma concentration-time profile from area under the curve (AUC), half-life ($t_{1/2}$), C_{max} and T_{max} .

Animal study

The *in-vivo* tissue distribution of DTX-NPs was evaluated by comparing with plain DTX. N-methyl nitroso urea (NMU) were subcutaneously inoculated to female Sprague Dawley rats at a dose 50 mg/kg body weight. Rats were euthanized by carbon dioxide asphyxiation and the presence of tumour was evaluated from the mammary glands. The rats with tumour were selected randomly and equally divided into three groups (n=5) as subjects. Two formulations, DTX-NPs and DTX injection were administered to the two groups at a 10 mg/kg dose via the tail vein, respectively. Then the rats were euthanized and blood sample were collected for assessing the pharmacokinetic profile of the formulation and plain DTX. Further, heart, liver, spleen, lung, kidney, mammary gland and tumour was collected, washed, weighed and homogenized (T25 Ultra-Turrax Homogenizer, IKA, Baden-Wurtemberg, Germany) in 1mL saline. 250 mL tissue homogenates was extracted by adding 250 mL methanol and 250 mL acetonitrile vortex-mixing the samples for 30 s (To analyze the bio-distribution of drug). The mixture was then centrifuged for 15 min at 25000 g, and the supernatant was transferred, filtered and injected into the HPLC system with paclitaxel as internal standard to determine DTX [29, 30].

Tumour inhibition study

The tumor size was measured using calipers, and the tumor volume was estimated by the formula: tumor volume (mm³) = (W×L) 2 ×1/2, where L is the length and W is the width of the tumor. Normally distributed data were represented as mean ± SD.

Statistical analysis

Statistical evaluation of data was performed using student's t-test or one-way ANOVA (GraphPadInStat software demo, La Jolla, CA), the evaluation data was used to assess the significance of differences. To compare the significance of the difference between the means of 2 groups, the Student's *t*-test was performed; in all cases, a value of $p < 0.05$ was accepted as significant. All the results are given, as mean ± standard deviation (SD).

Result and Discussion

The main aim of the work was to enhance the anticancer activity of DTX by forming a targeted delivery of NP using a targeting agent, hyaluronic acid. To enhance the concentration of drug delivery to the site of mammary carcinoma.

Hyaluronic acid were surface coupled with docetaxel loaded nanoparticles by forming a covalent bond between carboxylic groups of hyaluronic acid with amine group of chitosan forming an amide linkage in presence of EDC. To prevent particle-particle aggregation or extensive crosslinking of hyaluronic acid the EDC concentration was optimized.

The loading efficiency of DTX in NP's complex was considerably high (90.17 ± 4.19%) which confirms the high inclusion phenomenon between DTX and HA-CHI-NP (Table 1).

Preparation and characterization of Docetaxel-chitosan nanoparticles (DTX-CHI-NPs)

Particle size and surface charge of a delivery system are highly emphasized because of their importance in determine the fate of drug *in-vitro* and *in-vivo* release and distribution. Negatively charged delivery systems exhibit prolonged circulation time, high physical stability and avoid nonspecific cellular uptake. Particle sizes between 100 and 200nm have a favorable EPR (enhanced permeability and retention) effect on the tumour vasculature. The mean sizes of DTX-CHI-NP were within this range for optimal EPR effects. The average particle size of selected DTX-CHI-NP was 97.36 ± 3.07 nm ($p > .001$) and a relatively narrow size distribution having a polydispersity index of 0.05 (Figure 1(A)). The zeta potential was determined to measure the surface charges. The zeta potential of the HA-CHI-NP was found to be 31.34 ± 0.79 mV, which indicates high formulation stability [Figure 1(B); Table 1] [25, 26].

Table1. Physicochemical characterization of DTX and DTX-CHI-NP

Batch	Zeta Potential (-mV)	Particle Size (nm)	% EE	% Production yield
DTX	-25.28± 2.97	201.43 ± 1.94	-----	-----
DTX-CHI-NP	-31.34 ± 0.79	97.36 ± 3.07	90.17 ± 4.19	94.32 ± 2.52

All values are mean ± SD (n=5), * implies $p < 0.001$.

The crystalline properties of DTX and DTX-CHI-NP were evaluated by DSC and PXRD analysis. The DSC thermograms of DTX and DTX-CHI-NP are shown in figure 2A and 2B. DTX shows a distinct and sharp endothermic peaks at 230°C. However, DTX-CHI-NP

exhibited no peaks in the thermogram. The disappearance of DTX peak suggests that the drug might be completely encapsulated in the HA-CHI-NP or molecularly dispersed within the HA-CHI-NP [31].

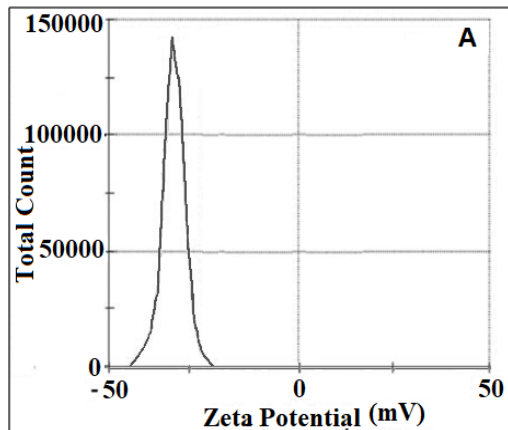


Figure 1A. Zeta potential of HA-CHI-NP.

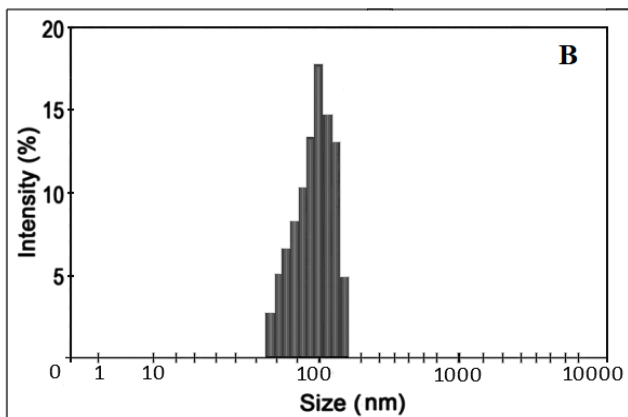


Figure 1B. Particle size of the DTX-CHI-NP.

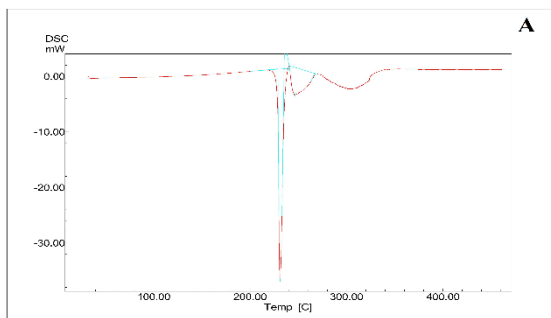


Figure 2A. DSC thermogram of DTX.

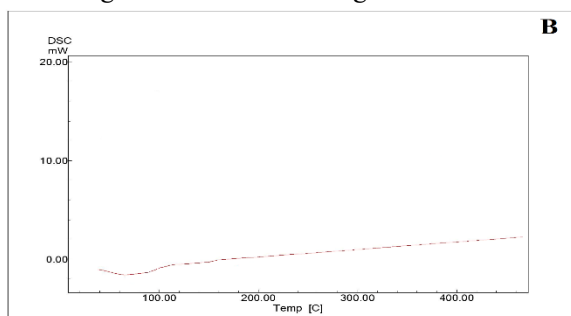


Figure 2B. DSC thermogram of DTX-CHI-NP.

The FTIR spectral peaks of DTX, HA-CHI-NP and DTX-CHI-NP were obtained.

The FTIR spectrum of chitosan shows a peaks at 1089 and 775.1 cm^{-1} which belongs to the saccharide structure of the chitosan. A strong amino peak at around 3433, 1591, and 1329.5 cm^{-1} were also observed. There is change in the IR peaks of $-\text{NH}_2$ and $-\text{OH}$ group stretching vibration in chitosan matrix obtained at 3429.1 cm^{-1} . In HA-CHI-NP a shift from 3427 to 3409 cm^{-1} is observed, and the peak of 3405.9 cm^{-1} was broaden, which manifest the enhancement of hydrogen bonding in the formation of NP. In NP the peak of 1598 cm^{-1} disappears and a new sharp peak at 1591.7 cm^{-1} appears, and the peak of amine bending vibrations shifted from 1598 cm^{-1} to 1528.1 cm^{-1} . The tripolyphosphoric groups of TPP are linked with ammonium group of chitosan by the inter- and intra-molecular action are enhanced in HA-CHI-NP. From IR spectrum of TPP, it is observed that vibration of the P-O at 1217.3 cm^{-1} was present. Amide group (1596 cm^{-1}) of CHI and P-O (1217.3 cm^{-1}) of TPP overlaps with 3156.3, 1662.6, 812 cm^{-1} of DTX-CHI-NP spectrum indicating that DTX may be loaded successfully to the HA-CHI-NPs. On comparing the IR spectrum of CHI and HA-CHI-NP following conjugation, additional peaks in the spectra of the HA-CHI-NP have been observed. A new peak appearing at 3430.4 cm^{-1} corresponded to bonded $-\text{NH}$ stretching vibrations. From the IR data it is clear that the HA coupled nanoparticles (HA-CHI-NP) had characteristic peaks of amide bond, which evidenced the successful coupling of hyaluronic acid group and the CHI amine group.

PXRD analysis was used to study the state of DTX in HA-CHI-NP. Figure 3A and 3B shows PXRD patterns of DTX and DTX-CHI-NP. The sharp diffraction peaks of DTX indicate a crystalline phase. The XRPD pattern of DTX shows the presence of intense, sharp peaks at 7.976, 11.669, 12.321, 16.276, 16.705, 22.099 and 22.995 on 2 θ scale which confirms its crystalline structure (Figure 3(A)). However the PXRD pattern of DTX-CHI-NP shows that all sharp peaks are subdued due to change into an amorphous state, suggesting complete encapsulation of drug in the HA-CHI-NP (Figure 3(B)).

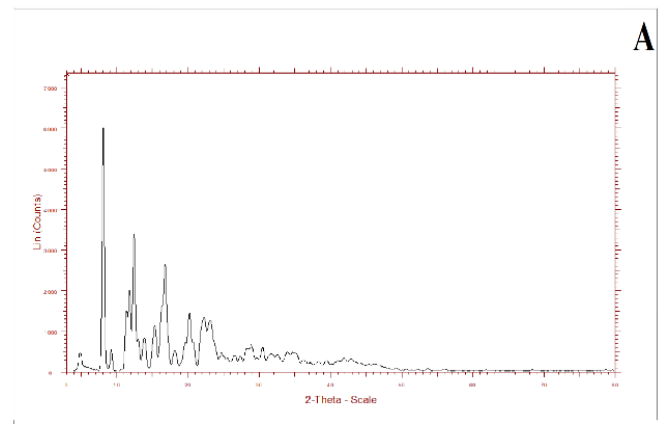


Figure 3A. PXRD pattern of DTX.

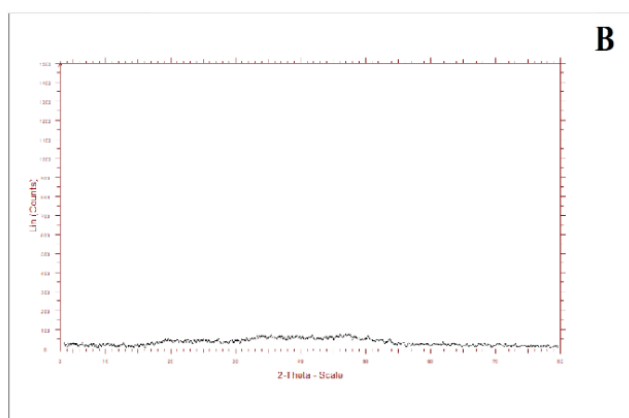


Figure 3B. PXRD pattern of DTX-CHI-NP.

SEM image of DTX-CHI-NP shows spherical particles (80–120 nm) (Figure 4).

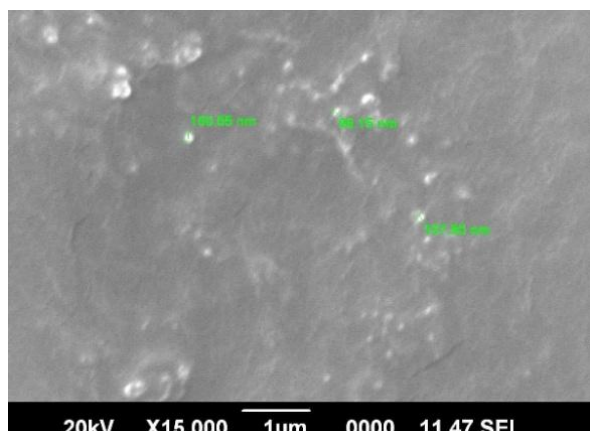


Figure 4. SEM image of DTX-CHI-NP.

In-vitro drug release study

The *in-vitro* release profile of DTX was compared with DTX-CHI-NPs. In the releasing medium DTX-NPs showed a sustained release for the following 60h (Figure 5). The total cumulative release of DTX and DTX-CHI-NP was found to be 98.5% in the end. As control groups, DTX injection showed a burst release in the first 4h and the total cumulative release reached the maximum (98.0%) in 12h. Although DTX-CHI-NPs showed high stability the release from the NP is sufficiently long compared to the traditional injection. It was also manifested that the NP shows sustained release of the drug which will lead to reduction in the dose. The slow and prolong release of DTX can reduce the peak concentration and prolong the therapeutic drug level [27].

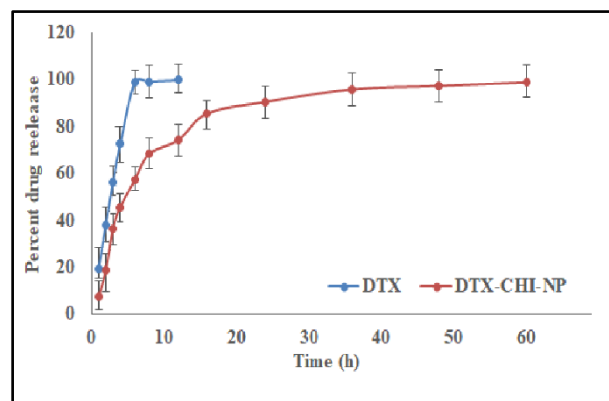


Figure 5. *In-vitro* percent drug release of DTX and DTX-CHI-NP (n=5).

In-vitro cytotoxicity study

To investigate the cytotoxicity of DTX-NPs in human breast adenocarcinoma cell line (MCF-7), MTT assay was performed. As shown in figure 6A, 6B and 6C, a dose dependent cytotoxicity was observed. With the increase of concentration, the cytotoxicity of DTX-CHI-NPs increased, ranging from 5 to 100 $\mu\text{g/mL}$. DTX-CHI-NPs displayed relatively highly significant cell inhibition as compared to DTX, indicating higher cytotoxicity. The HA coupled DTX-CHI-NP showed significant cytotoxic effect than plain DTX after 24, 48 and 72h of incubation period in MCF-7 cell lines ($p < 0.05$). The HA coupled DTX-CHI-NP showed a significant difference in reduction of cell viability than plain DTX (Figure 6A, 6B and 6C). The 50% of growth inhibition (IC_{50}) of HA coupled DTX-CHI-NP was much lower than plain DTX. It was observed that HA coupled DTX-CHI-NP showed increase in cytotoxicity from 10.05 ± 4.08 at 24h to 2.18 ± 2.97 $\mu\text{g/mL}$ at 72h. However the IC_{50} values of DTX was found to be 110.21 ± 4.29 at 24h to 50.26 ± 3.82 $\mu\text{g/mL}$ at 72h (Table 2). The HA coupled DTX-CHI-NP enhanced the cytotoxicity of DTX about 25.09-fold on MCF-7 cell compared with to plain DTX. Out-fluxing of the drugs from the cells is a major reason of multidrug resistance, through *p*-glycoprotein resulted in decreasing the intracellular concentration of drug. NP's can greatly increase the amount of drug delivered intracellularly into cells by endocytosis, the cells were more vulnerable to the cytotoxic effect of drug [32]. The direct interaction between drug and cells could be reduced by loading drug into the core of polymeric NPs. Hence it can be demonstrate that DTX-CHI-NP strongly enhances the cytotoxic effect of the DTX against breast cancer in terms of sustained and targeted delivery of drug.

Table 2. IC_{50} values ($\mu\text{g/ml}$) of DTX and DTX-CHI-NP at different time points with MCF-7 cell lines

Formulation	24h	48h	72h
DTX ($\mu\text{g/ml}$)	110.21 ± 4.29	100.23 ± 3.74	50.26 ± 3.82
DTX-CHI-NP ($\mu\text{g/ml}$)	10.05 ± 4.08	7.42 ± 3.58	$2.18 \pm 2.97^*$

All values are mean \pm SD (n=5), * implies $p < 0.001$

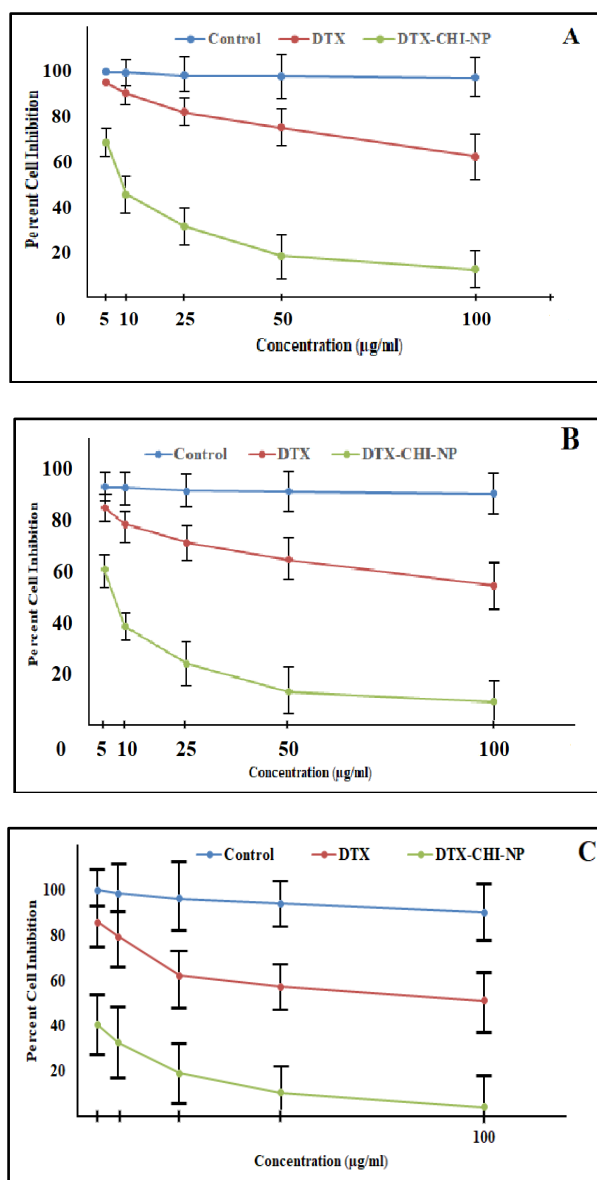


Figure 6. In-vitro cytotoxicity study of DTX and DTX-CHI-NP on MCF-7 cell line at different time intervals at a concentration of 5, 10, 25, 50 and 100µg/ml; Figure: 6A- Indicate the cytotoxic behavior at 24h, Figure: 6B- Indicate the cytotoxic activity at 48h, Figure: 6C- Indicate the cytotoxic activity at 72h.

Pharmacokinetic study

The pharmacokinetic profiles of DTX and HA coupled DTX-CHI-NP in SD rats were investigated.

As shown in Figure 7 and Table 3, the AUCs of DTX after administration of plain DTX and HA coupled DTX-CHI-NP were 668.42 ± 3.79 and 6521.85 ± 10.08 µg/L-h, respectively, which increased 11.2 fold. The half-life of DTX in DTX and HA coupled DTX-CHI-NP were nearly 10.53 times longer than that of plain DTX. All the results indicated that on the one hand HA coupled DTX-CHI-NP greatly prolong the blood circulation time of DTX and improve the bioavailability of DTX.

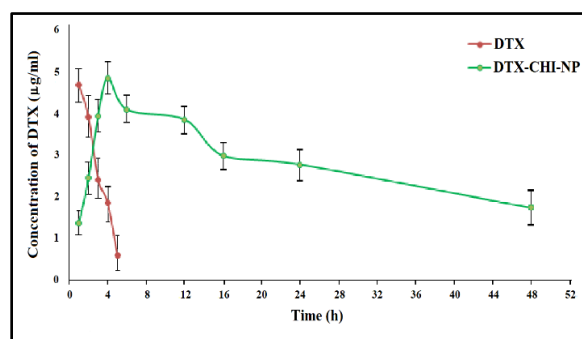


Figure 7. *In-vivo* pharmacokinetic profile of DTX and DTX-CHI-NP (n=5). All values are mean \pm SD (n=5), * implies $p < 0.001$.

Table 3. Pharmacokinetic parameters of DTX and DTX-CHI-NP

Parameters	DTX	DTX-CHI-NP
C_{max} (µg/ml)	4.68 ± 2.59	4.89 ± 1.27
T_{max} (h)	1.0 ± 2.84	$5.6 \pm 1.34^*$
$t_{1/2}$ (h)	3.374 ± 2.63	$35.52 \pm 3.97^*$
AUC (h.µg/mL)	668.42 ± 3.79	6521.85 ± 10.08

All values are mean \pm SD (n=5), * implies $p < 0.001$.

Biodistribution

To compare the targeting ability of NP distribution of drug was assessed after intravenous administration of DTX and HA coupled DTX-CHI-NP by determining the mean DTX contents of heart, liver, spleen, lung, kidney and tumor at 24 h as shown in Figure 8. For HA coupled DTX-CHI-NPs group, 71.084 µg/g DTX were distributed in tumor, while for plain DTX group, only 22.002 µg/g. The significant difference was observed in tumor accumulation of drug, representing tumor targeted effect of HA coupled DTX-CHI-NP. This may increase the therapeutic potential of DTX with reduced systemic toxicity and enhanced antitumor efficacy. It was also reported that the drug was not present in the brain tissue. Also the drug gets distributed to other organs in DTX group in a sufficient quantity. The targeting effect of the HA coupled DTX-CHI-NP might be due to the HA receptors on the surfaces of the tumour cells of the breast (HA receptors such as CD44 and RHAMM/HMMR) which might bind with the HA coupled with the NP.

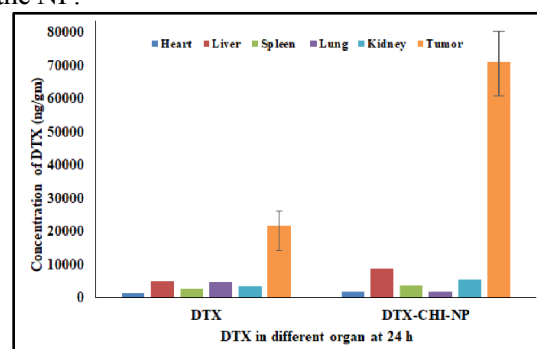


Figure 8. Biodistribution of DTX and DTX-CHI-NP on female Sprague Dawley rats at 24h in different organs such as heart, liver, spleen, lung, kidney and tumour.

Tumour inhibition study

The tumour inhibition effect was assessed by analyzing the decrease in the tumour volumes after administration of DTX and HA coupled DTX-CHI-NP after development of the tumour. The tumor volume increased rapidly from the initial average volume on day 28. In plain DTX groups, the tumor decreases slower than the control group, whose volumes were 287.39 and 193.89 mm³. A significant tumor inhibition was observed in HA coupled DTX-CHI-NP group (Figure 9). On day 28, the tumor volumes were only 25.21 mm³. HA coupled DTX-CHI-NP exhibited an extreme significant tumor inhibition rate (91.69%). HA coupled DTX-CHI-NP displayed more significant tumour inhibition than plain DTX may be due to: (1) HA coupled DTX-CHI-NP can accumulate in tumor due to the EPR effects, which significantly increases the amount of DTX in tumor tissue; (2) The targeting behavior of the NP which was coupled with the hyaluronic acid to target the HA receptor located at the developing breast tumour. Therefore, HA coupled DTX-CHI-NP can be highly efficiently transported into tumor.

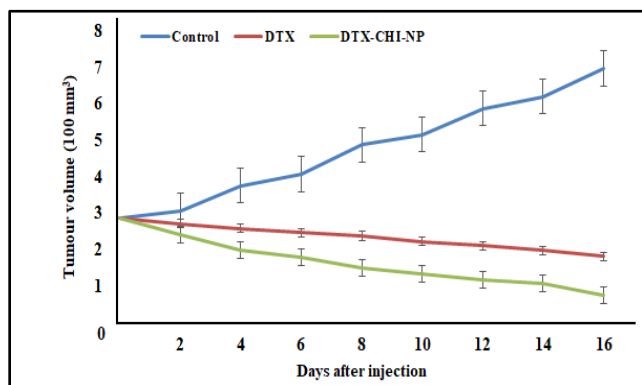


Figure 9. In vivo antitumor efficacy of DTX-CHI-NPs. Tumour volumes of breast carcinoma, plain DTX and DTX-CHI-NPs. Each data point is represented as mean \pm SD (n=5) (*p<0.05; **p<0.01).

Conclusion

In summary, the HA coupled DTX-CHI-NP were synthesized by ionotropic gelation method for the targeted delivery of DTX to the breast cancer. Nanoparticles synthesis eliminated the complicated preparation procedure and toxic residual solvents in common preparation method. HA coupled DTX-CHI-NP were produced efficiently with high yield, drug loading and high encapsulation efficiency were also achieved. The resulting DTX-CHI-NPs displayed high stability and significantly higher cytotoxicity compared to plain DTX on MCF-7 cell line. The antitumor effects of DTX-CHI-NPs were higher than that of plain DTX, which might be due to the passive targeting ability of DTX-CHI-NPs to tumor tissue. The results showed that HA coupled DTX-CHI-NP is therefore anticipated to be promising carriers for the targeting of breast tumors.

Declaration of interest

The authors report no declarations of interest.

Acknowledgement

The authors are thankful to Cipla Pvt Ltd (Mumbai, India) for providing gift samples of Erlotinib hydrochloride. Authors are thankful to Ms. Fatma Rafiq Zakaria, Chairman of Maulana Azad Educational Trust, Aurangabad (India) for providing the necessary infrastructure facilities. Special thanks to Dr. Ayaz Ali, Associate Professor, Y.B Chavan college of Pharmacy, Aurangabad (India) for his assistance in performing, Pharmacokinetic and biodistribution studies. Momin Mufassir is also thankful to University Grants Commission (UGC), New Delhi and Ministry of Minority Affairs (MOMA) for financial assistance.

References

- Suarato G, Li W, and Meng Y: Role of pH-responsiveness in the design of chitosan-based cancer nanotherapeutics: A review. *Bio interphases*. 2016; doi:10.1116/1.4944661.
- Arola OJ, Saraste A, Pulkki K, Kallajoki M, Parvinen M, Voipio-Pulkki LM: Acute doxorubicin cardiotoxicity involves cardiomyocyte apoptosis. *Cancer Res* 2000; 60: 1789-1792.
- Liu B, Yang M, Li R, Ding Y, Qian X, Yu L, Jiang X: The antitumor effect of novel docetaxel-loaded thermosensitive micelles. *Eur J Pharm Biopharm* 2008; 69: 527-534.
- Tammam SN, Azzazy HM, Lamprecht A. Biodegradable particulate carrier formulation and tuning for targeted drug delivery. *J Biomed Nanotechnol* 2015; 11: 555-577.
- Gao H, Cao S, Yang Z, Zhang S, Zhang Q, Jiang X: Preparation, characterization and anti-glioma effects of docetaxel-incorporated albumin-lipid nanoparticles. *J Biomed Nanotechnol* 2015; 11: 2137-2147.
- Nukolova NV, Oberoi HS, Cohen SM, Kabanov AV, Bronich TK: Folate-decorated nanogels for targeted therapy of ovarian cancer. *Biomaterials* 2011; 32:5417-5426.
- Talelli M, Iman M, Varkouhi AK, Rijcken CJ, Schiffelers RM, Etrych T, Ulbrich K, van Nostrum CF, Lammers T, Storm G, Hennink WE: Core-crosslinked polymeric micelles with controlled release of covalently entrapped doxorubicin. *Biomaterials* 2010; 31: 7797-7804.
- Huang W-T, Larsson M, Wang Y-J, Chiou S-H, Lin H-Y, and Liu D-M: Demethoxy curcumin-Carrying Chitosan-Antibody Core-Shell Nanoparticles with Multi therapeutic Efficacy toward Malignant A549 Lung Tumor: From in Vitro Characterization to in Vivo Evaluation. *Mol. Pharmaceutics*. Doi: 10.1021/mp500747w.
- Jiang Y, Yang N, Zhang H, Sun B, Hou C, Ji C, Zheng J, Liu Y, Zuo P: Enhanced in vivo antitumor efficacy of dual-functional peptide-modified docetaxel nanoparticles through tumor targeting and Hsp90 inhibition. *Journal of Controlled Release* 2016; 221: 26-36.
- Akima K, Ito H, Iwata Y, Matsuo K, Watari N, Yanagi M, Hagi H, Oshima K, Yagita A, Atomi Y, Tatekawa I: Evaluation of antitumor activities of hyaluronate binding antitumor drugs: synthesis, characterization and antitumor activity. *J. Drug Target* 1996; 4: 1-8.
- Luo Y, Prestwich GD: Synthesis and selective cytotoxicity of a hyaluronic acid-antitumor bioconjugate. *Bioconjug. Chem.* 1999; 10: 755-763.
- Peterson RM, Yu Q, Stamenkovic I, Toole BP: Perturbation of hyaluronan interactions by soluble CD44 inhibits growth of murine mammary carcinoma cells in ascites. *Am. J. Pathol.* 2000; 156: 2159-2167.
- Jain A & Jain SK: In vitro and cell uptake studies for targeting of ligand anchored nanoparticles for colon tumour. *European journal of pharmaceutical sciences* 2008; 35: 404-416.
- Weiss RB, Donehower RC, Wiernik PH: Hypersensitivity reactions from taxol. *J. Clin. Oncol.* 1990; 8: 1263-1268.
- Kraynak MA: Pharmaceutical aspects of docetaxel. *Am. J. Health Syst. Pharm.* 1997; S7-S10.
- Immordino ML, Brusa P, Arpicco S: Preparation, characterization, cytotoxicity and pharmacokinetics of liposomes containing docetaxel. *J. Control Release* 2003; 91: 417-429.

17. Alexopoulos A, Karamouzis MV, Stavrinides H: Phase II study of pegylated liposomal doxorubicin (caelyx) and docetaxel as first-line treatment in metastatic breast cancer. *Ann. Oncol.* 2004; 15: 891-895.
18. Grosse PY, Bressolle F, Pinguet F: In vitro modulation of doxorubicin and docetaxel antitumoral activity by methyl- β -cyclodextrin. *Eur. J. Cancer* 1998; 34:168-174.
19. He Y, Li P, Yalkowsky SH: Solubilization of fluasterone in cosolvent/cyclodextrin combinations. *Int. J. Pharm.* 2003; 264: 25-34.
20. Yalkowsky SH, Roseman TJ: Solubilization of drugs by co-solvents. In: Yalkowsky, S.H. (Ed.), *Techniques of Solubilization of Drug*. Marcel Dekker Inc, New York, NY. 1981; 91-134.
21. Kawakami K, Miyoshi K, Ida Y: Solubilization behavior of poorly soluble drugs with combined use of Gelucire 44/14 and cosolvent. *J. Pharm. Sci.* 2004; 93:1471-1479.
22. Parka M-O, Keuma C-G, Song J-Y, Kim D, Cho C-W: A novel aqueous parenteral formulation of docetaxel using pro drugs. *International Journal of Pharmaceutics* 2014; 462:1-7.
23. Kiill CP, Barud H dS, Santagneli SH, Ribeiro SJL, Silva AM, Tercjak A, Gutierrez J, Pironi AM, Gremião MPD: Synthesis and factorial design applied to a novel chitosan/sodium polyphosphate nanoparticles via ionotropic gelation as an RGD delivery system. *Carbohydrate Polymers* 2016; doi:10.1016/j.carbpol.2016.11.053.
24. Calvo P, Remuñán-López C, Vila-Jato JL & Alonso MJ: Novel hydrophilic chitosan-polyethylene oxide nanoparticles as protein carriers. *Journal of Applied Polymer Science* 1997; 63(1): 125-132.
25. Momin MM, Zaheer Z, Zainuddin R & Sangshetti J.N: Extended release delivery of erlotinib glutathione nanosponge for targeting lung cancer. *Artificial Cells, Nanomedicine, and Biotechnology* 2017; doi: 10.1080/21691401.2017.1360324.
26. Zainuddin R, Zaheer Z, Sangshetti JN & Momin MM: Enhancement of oral bioavailability of anti-HIV drug Rilpivirine HCl through nanosponge formulation. *Drug Development and Industrial Pharmacy* 2017; doi: 10.1080/03639045.2017.1371732.
27. Tang X, Wang G, Shi R, Jiang K, Meng L, Ren H, Wu J and Hu Y: Enhanced tolerance and antitumor efficacy by docetaxel-loaded albumin nanoparticles 2015; doi: 10.3109/10717544.2015.1049720.
28. Gupta Y, Jain A, Jain P, Jain SK: Design and development of folate appended liposomes for enhanced delivery of 5-FU to tumor cells. *J. Drug Target* 2007; 15(3): 231-240.
29. Perše M, Cerar A, Injac R & Štrukelj B: N-methylnitrosourea Induced Breast Cancer in Rat, the Histopathology of the Resulting Tumours and its Drawbacks as a Model. *Pathol. Oncol. Res.* 2009; 15:115-121.
30. Hu Q, Rijcken CJ, Bansal R, Hennink WE, Storm G, Prakash J: Complete regression of breast tumour with a single dose of docetaxel-entrapped core-cross-linked polymeric micelles. *Biomaterials* 2015; 53:370e378.
31. Lembo D, Swaminathan S, Donalisio M, Civra A, Pastero L, Aquilano D, Vavia P, Trotta F, Cavalli R: Encapsulation of Acyclovir in new carboxylated cyclodextrin-based nanosponges improves the agent's antiviral efficacy. *International Journal of Pharmaceutics* 2013; 443: 262-272.
32. Yoo HS, Park TG: Biodegradable polymeric micelles composed of doxorubicin conjugated PLGA-PEG block copolymer. *J. Controlled Release* 2001; 70: 63-70.